

Supporting Information

High-Current-Density, Long-Duration Cycling of Soluble Organic Active Species for Non-Aqueous Redox Flow Batteries

Jarrold D. Milshtein,^{a,b,§} Aman Preet Kaur^{c,§}, Matthew D. Casselman,^c Jeffrey A. Kowalski,^{a,d} Subrahmanyam Modekrutti,^c Peter L. Zhang,^c N. Harsha Attanayake,^c Corrine F. Elliott,^c Chad Risko,^{c,e} Sean R. Parkin,^c Fikile R. Brushett,^{a,d*} Susan A. Odom^{c*}

^a Joint Center for Energy Storage Research, USA

^b Department of Materials Science and Engineering, Massachusetts Institute of Technology, Cambridge, MA 02139 USA

^c Department of Chemistry, University of Kentucky, Lexington, KY 40506 USA

^d Department of Chemical Engineering, Massachusetts Institute of Technology, Cambridge, MA 02139 USA

^e Center for Applied Energy Research, University of Kentucky, Lexington, KY 40511 USA

Contents

1. Nuclear Magnetic Spectroscopy of New Neutral Compounds p.3

Figure S1. ¹H NMR spectrum of MEPT in CDCl₃.

Figure S2. ¹³C NMR spectrum of MEPT in CDCl₃.

Figure S3. ¹H NMR spectrum of MEEPT in CDCl₃.

Figure S4. ¹³C NMR spectrum of MEEPT in CDCl₃.

2. Electron Paramagnetic Resonance Spectroscopy of Radical-Cation Salts p.7

Figure S5. EPR spectra of (a) EPT-BF₄, (b) MEPT-BF₄, and (c) MEEPT-BF₄ salts in dichloromethane.

3. UV-vis Study of Radical-Cation Decay p.8

3.1. Decay Study in Acetonitrile p.8

Figure S6. Normalized intensity of UV-vis absorbance at 514 nm vs. time of 0.15 mM (a) EPT-BF₄, (b) MEPT-BF₄, and (c) MEEPT-BF₄ in ACN.

3.2. Decay Study in Propylene Carbonate p.9

Figure S7. UV-vis spectra of (a) EPT-BF₄, (b) MEPT-BF₄, and (c) MEEPT-BF₄ at 0.15 mM in PC, recorded at 0, 1, 3, 5, and 24 h after dissolution. Characteristic peaks appear at 317, 446, 515, 758, and 853 nm. Normalized intensity of UV-vis absorbance at 515 nm vs. time for 0.15 mM (d) EPT-BF₄, (e) MEPT-BF₄, and (f) MEEPT-BF₄ in PC.

4. Cyclic Voltammetry p.10

4.1. Cyclic Voltammetry with Ferrocene Reference and of the Full Potential Window p.10

Figure S8. Cyclic voltammograms (cycle 1) of EPT (blue, top), MEPT (red, middle), and MEEPT (black, bottom) at 1 mM in 0.1 M TEABF₄ / ACN. (a) First positive couple of each active species with ~ 0.7 mM ferrocene internal reference. (b) Full

[§]These authors contributed equally.

*Corresponding author. Email address: brushett@mit.edu (F. R. Brushett)

**Corresponding author. Email address: susan.odom@uky.edu (S. A. Odom)

potential window of the organic active species, indicating additional irreversible couples at 0.8 – 1.0 V vs. Fc/Fc⁺.

4.2. Cyclic-Voltammetry Scan-Rate Study *p.11*

Figure S9. CV scan-rate dependence study for (a) EPT, (b) MEPT, and (c) MEEPT, and Randles-Sevcik construction (peak current vs. square root of scan rate) for the oxidative (anodic) waves of (d) EPT, (e) MEPT, and (f) MEEPT.

5. Bulk Electrolysis *p.12*

5.1. Bulk-Electrolysis Cell Schematic *p. 12*

Figure S10. Photograph of the bulk-electrolysis cell, with relevant ports and electrodes labeled.

5.2. Potential vs. Capacity *p.13*

Figure S11. Potential vs. capacity curves from bulk-electrolysis experiments showing cycles 2, 5, and 10 for each of (a) EPT, (b) MEPT, and (c) MEEPT at 5 mM in 1 M TEABF₄ / ACN. Theoretical capacities are 0.134 Ah L⁻¹ (0.469 mAh) for each experiment, and 10 cycles completed in 7 h.

5.3. Cyclic Voltammograms Before and After Cycling *p.14*

Figure S12. Cyclic voltammograms (cycle 2) before and after 10 bulk-electrolysis cycles for (a) EPT, (b) MEPT, and (c) MEEPT at 5 mM in 1 M TEABF₄ / ACN.

5.4. Quantitative Cyclic Voltammetry Analysis Before and After Cycling *p.15*

Table S1: Quantitative CV characteristics of EPT, MEPT, and MEEPT before and after bulk electrolysis cycling. Tabulated values are calculated from the data available in Figure S12.

6. Image of Assembled Flow Cell *p.16*

Figure S13. Photograph of the assembled flow cell, connected to the pump and reservoirs.

1 Nuclear Magnetic Resonance Spectroscopy

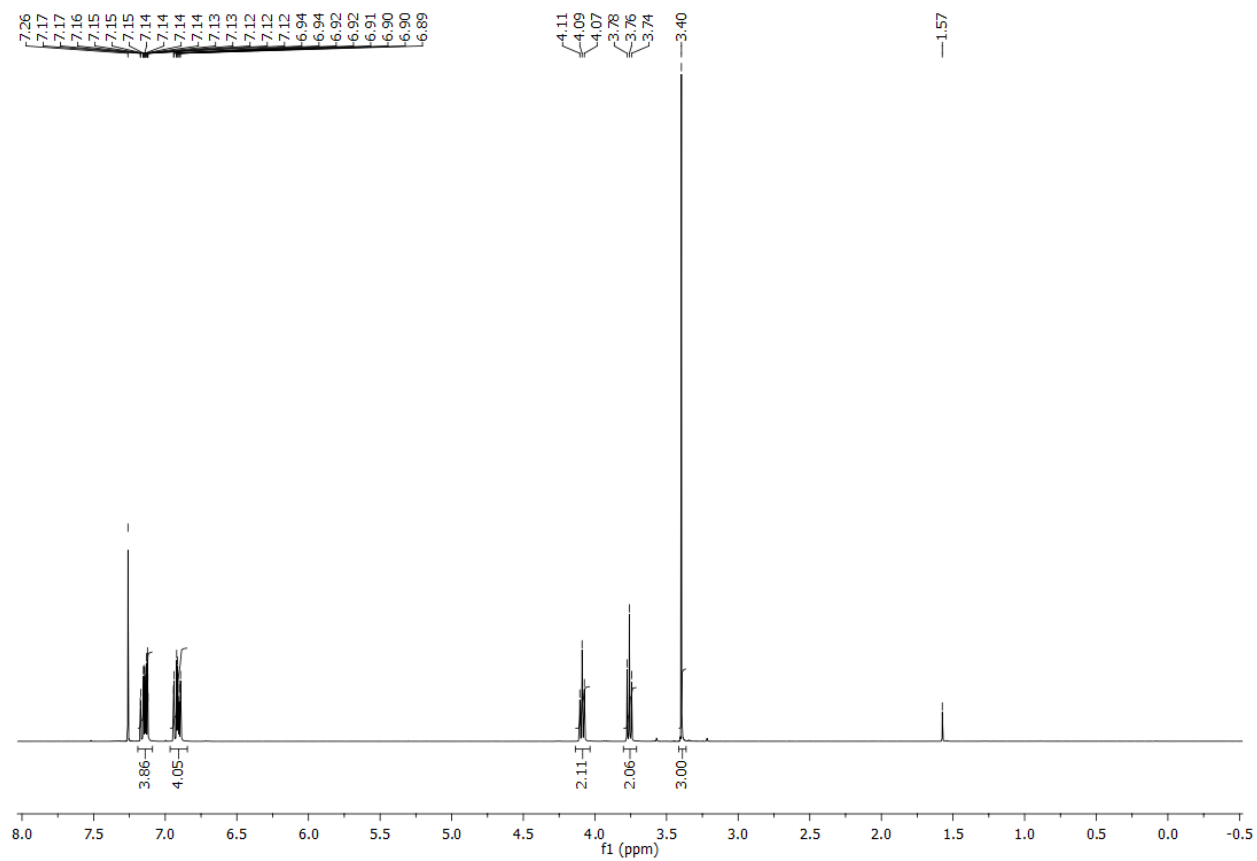


Figure S1. ^1H NMR spectrum of MEPT in CDCl_3 .

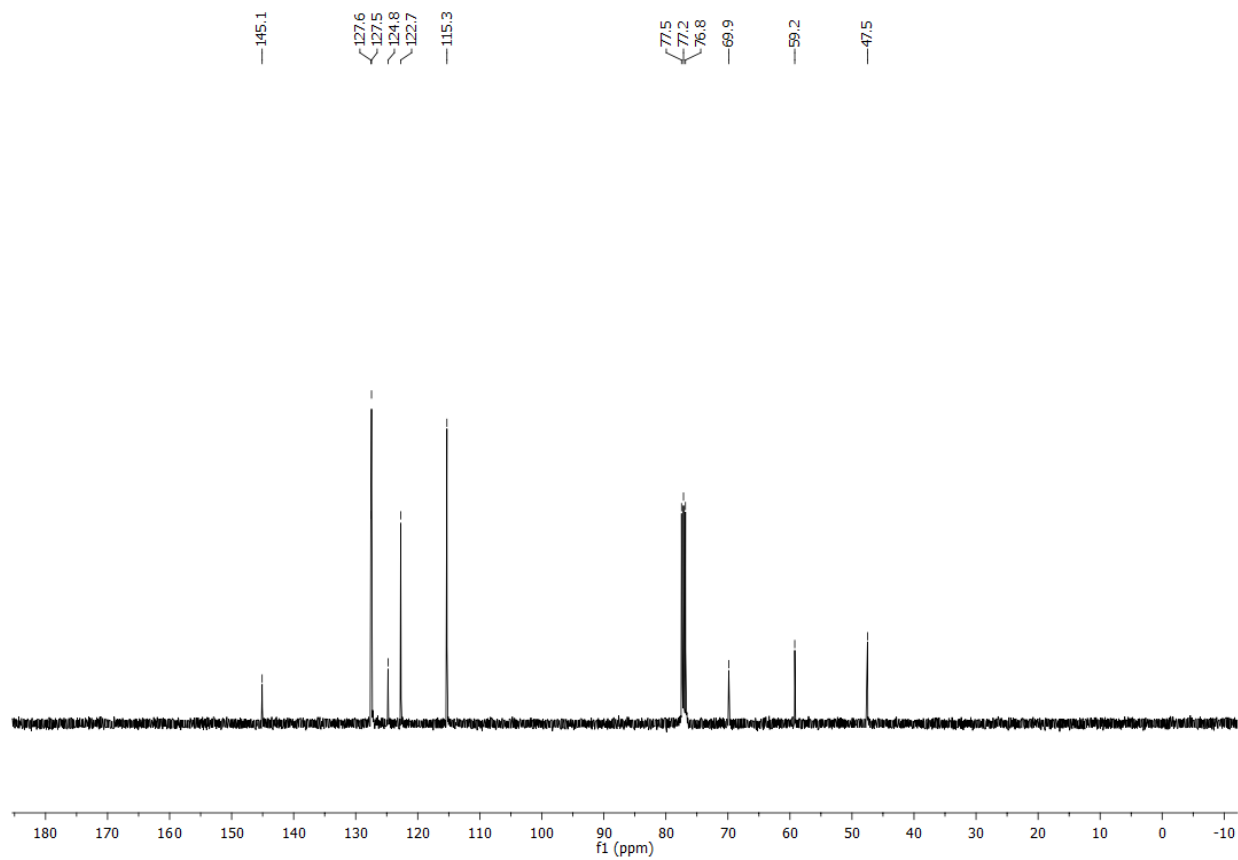


Figure S2. ^{13}C NMR spectrum of MEPT in CDCl_3 .

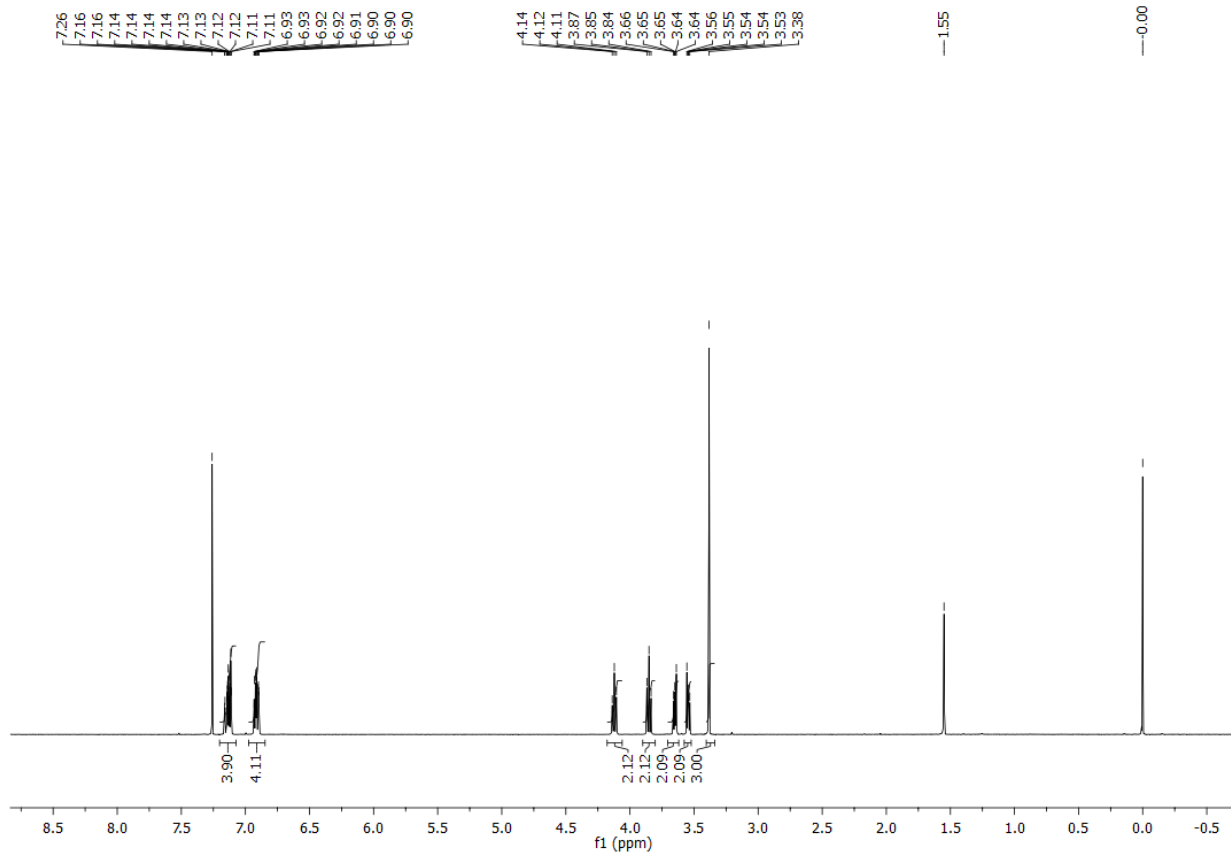


Figure S3. ^1H NMR spectrum of MEEPT in CDCl_3 .

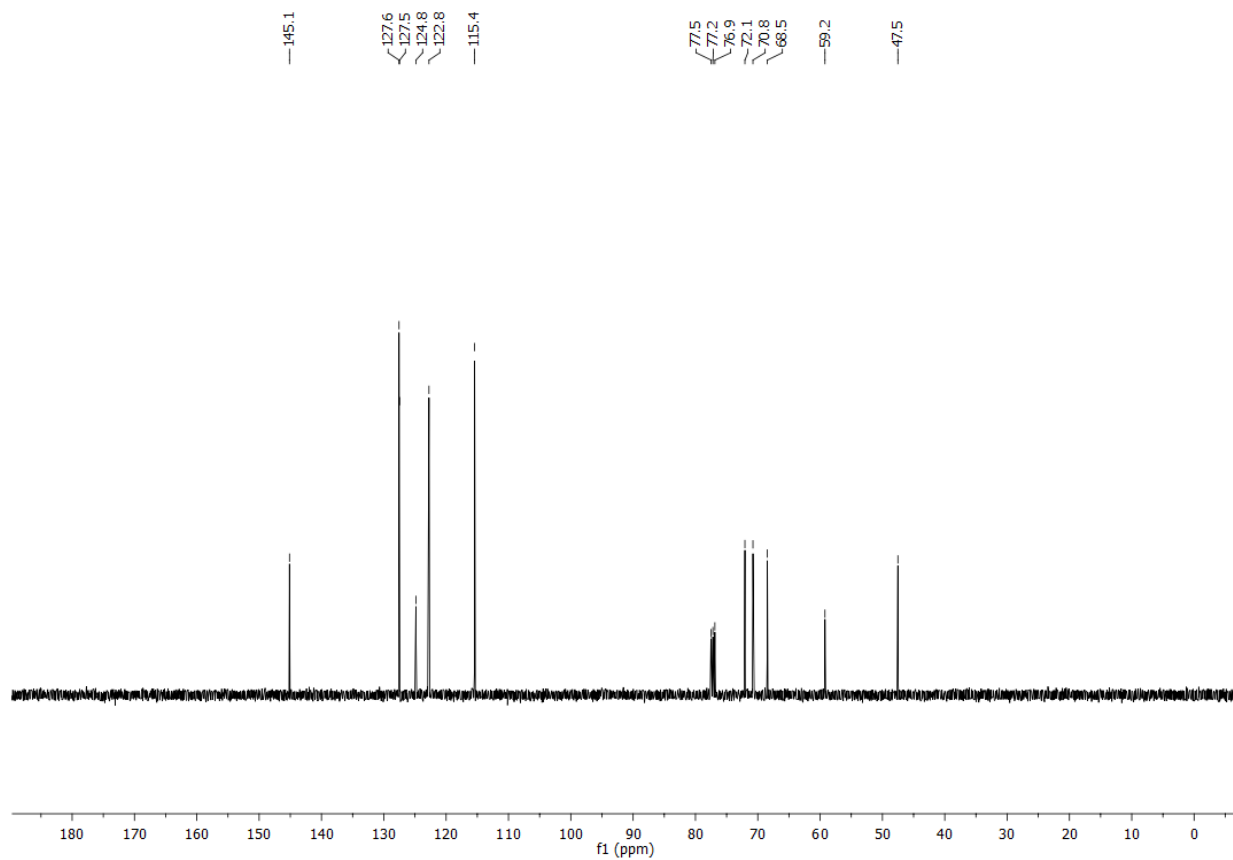


Figure S4. ^{13}C NMR spectrum of MEEPT in CDCl_3 .

2 Electron Paramagnetic Resonance Spectroscopy of Radical-Cation Salts

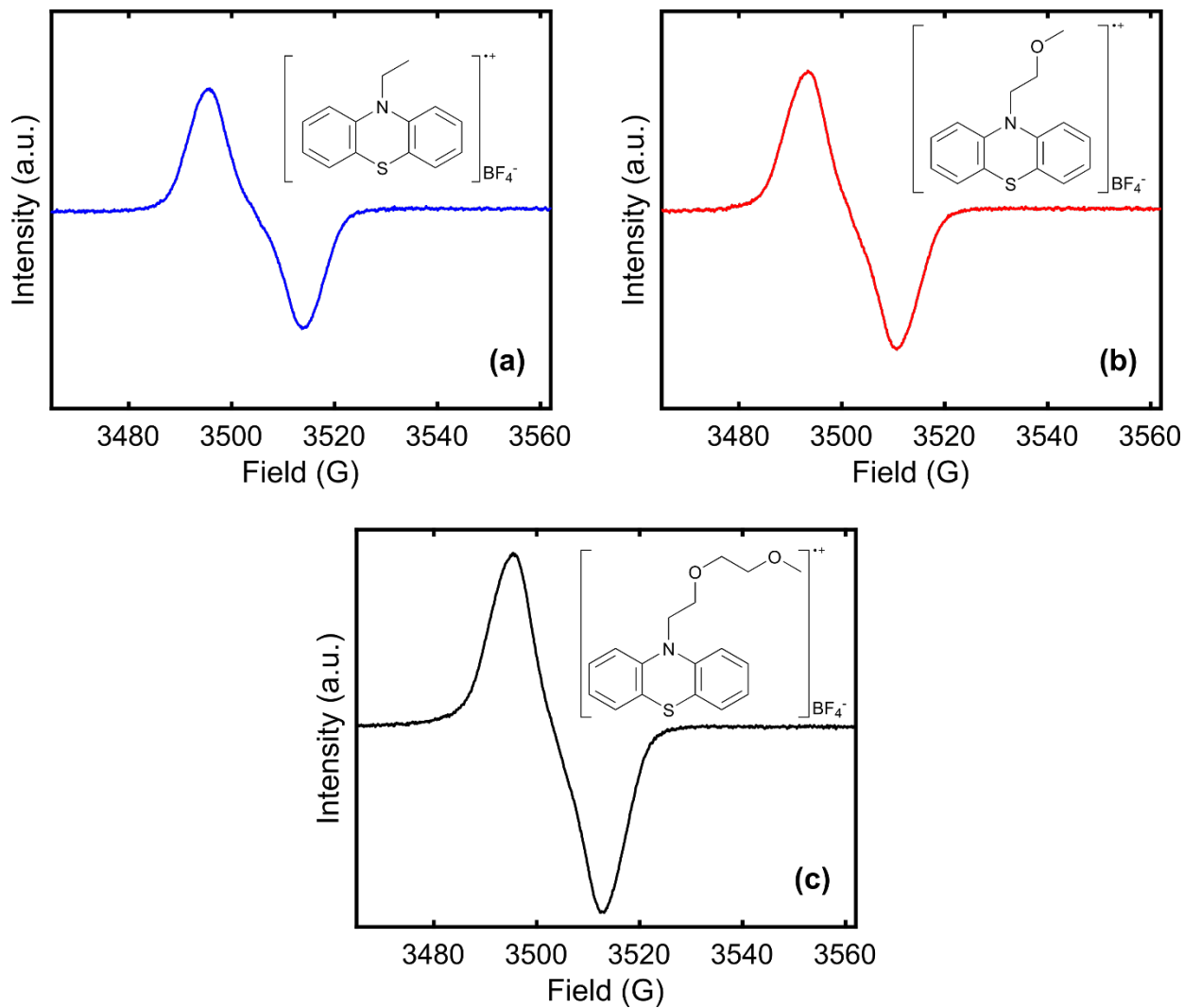


Figure S5. EPR spectra of (a) EPT-BF₄, (b) MEPT-BF₄, and (c) MEEPT-BF₄ salts in dichloromethane.

3 UV-vis Study of Radical-Cation Decay

3.1 Decay Study in Acetonitrile

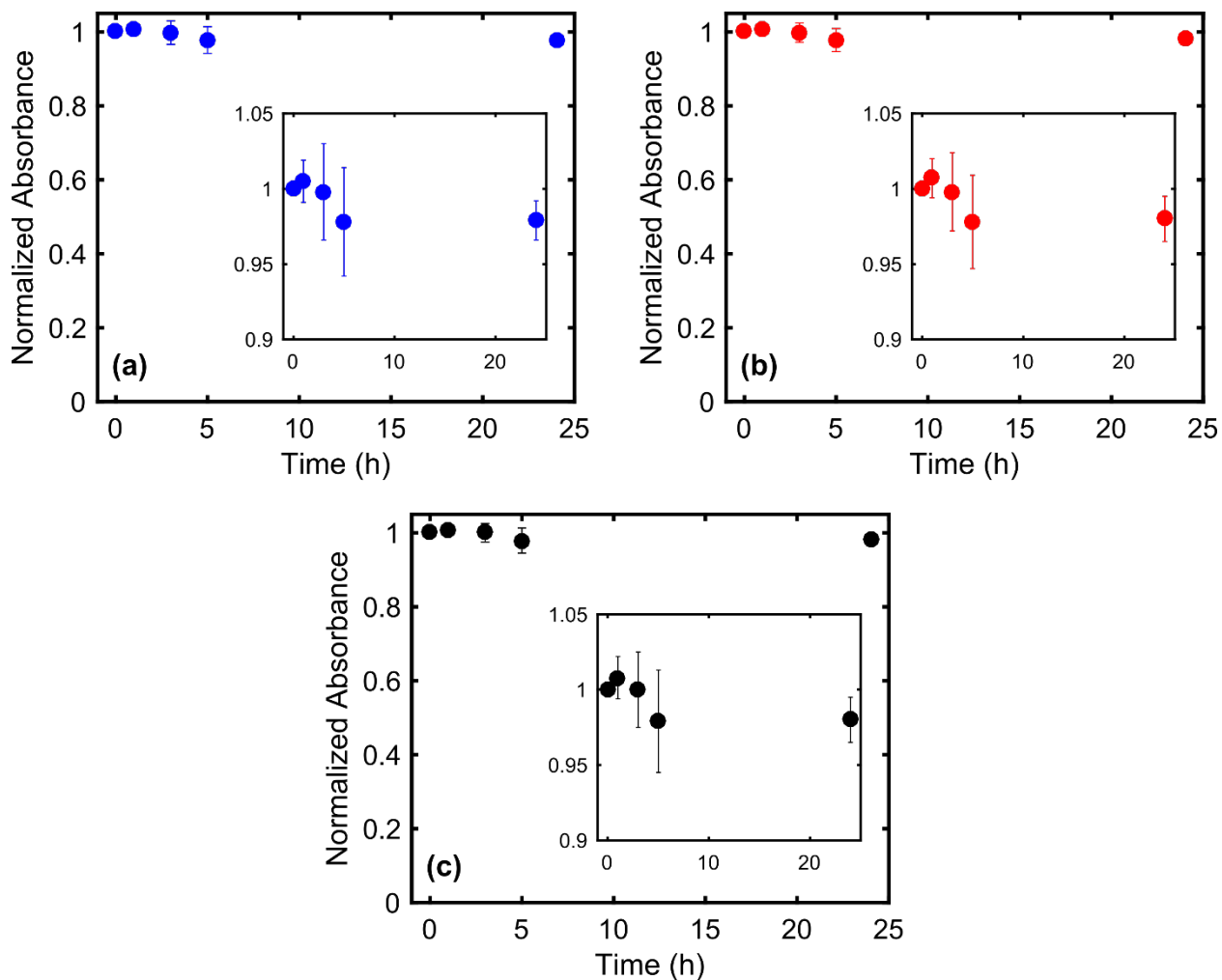


Figure S6. Normalized intensity of UV-vis absorbance at 514 nm vs. time of 0.15 mM (a) EPT-BF₄, (b) MEPT-BF₄, and (c) MEEPT-BF₄ in ACN. Inset: data expanded between absorbance values of 0.9-1.05, recorded at 0, 1, 3, 5, and 24 h after dissolution.

3.2 Decay Study in Propylene Carbonate

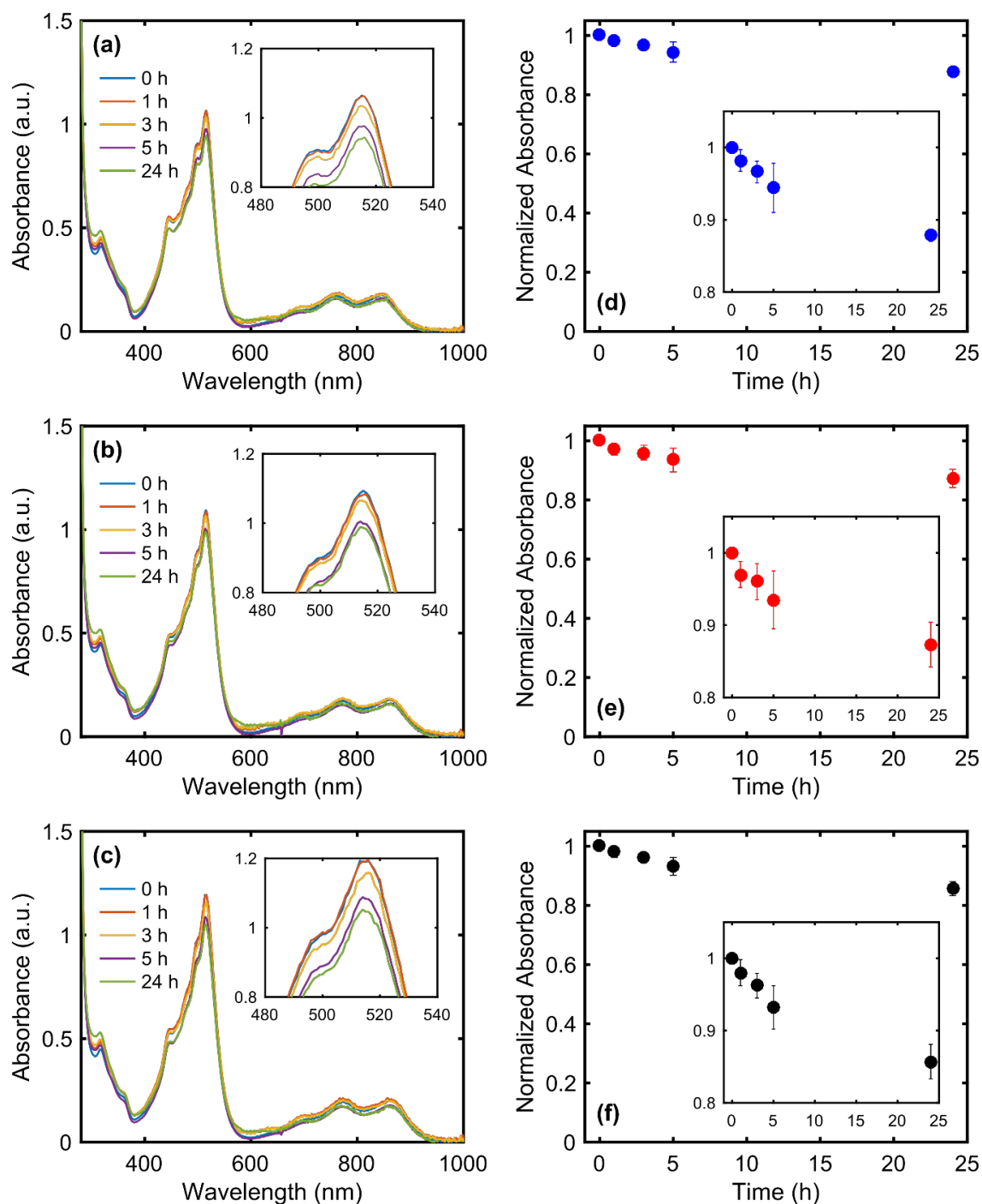


Figure S7. UV-vis spectra of (a) EPT-BF₄, (b) MEPT-BF₄, and (c) MEEPT-BF₄ at 0.15 mM in PC, recorded at 0, 1, 3, 5, and 24 h after dissolution. Characteristic peaks appear at 317, 446, 515, 758, and 853 nm. Normalized intensity of UV-vis absorbance at 515 nm vs. time for 0.15 mM (d) EPT-BF₄, (e) MEPT-BF₄, and (f) MEEPT-BF₄ in PC. Insets for a-c: expansion of most intensely absorbing peak. Insets for d-f: data expanded for absorbance values between 0.8-1.05.

4 Cyclic Voltammetry

4.1 Cyclic Voltammetry with Ferrocene Reference and of the Full Potential Window

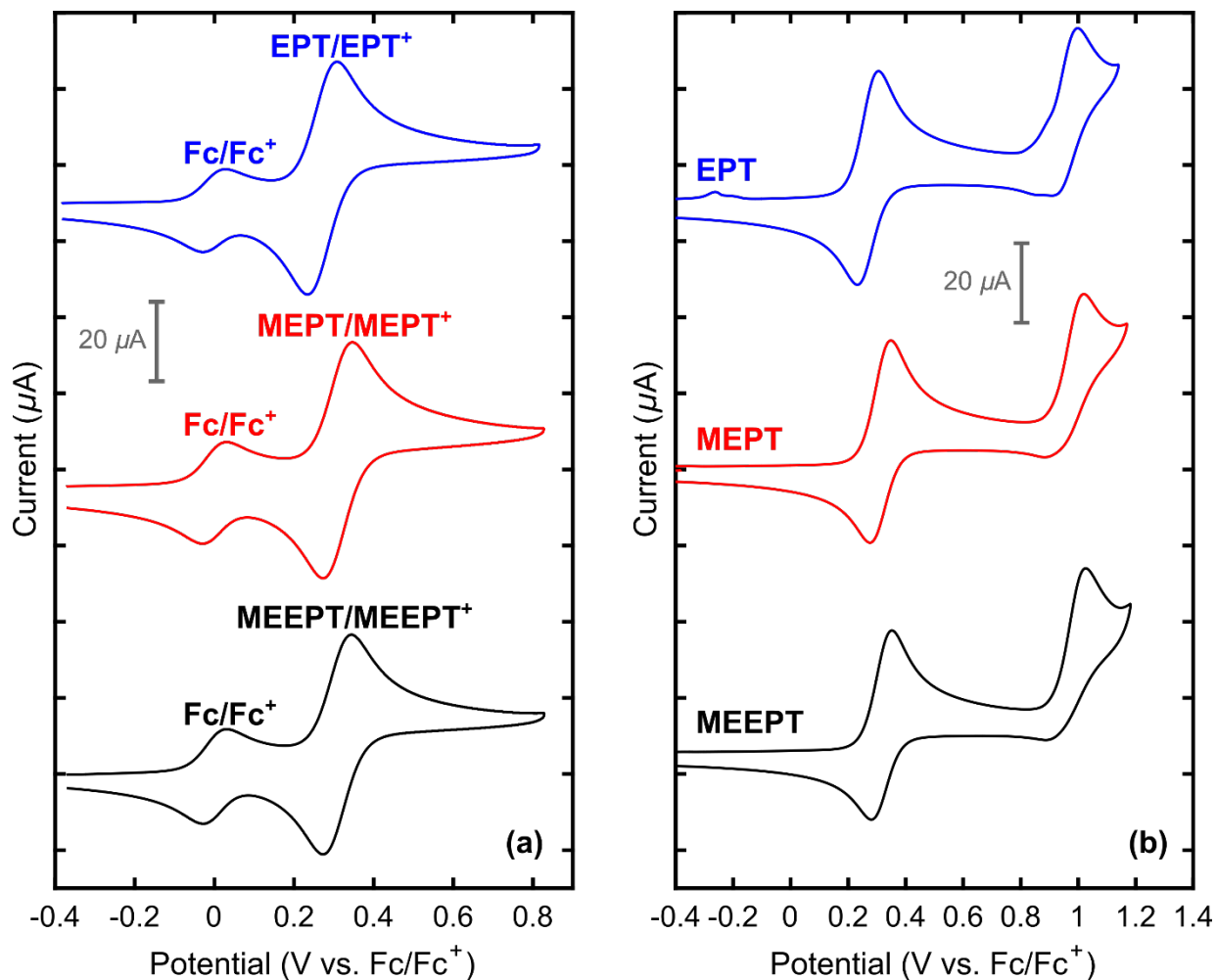


Figure S8. Cyclic voltammograms (cycle 1) of EPT (blue, top), MEPT (red, middle), and MEEPT (black, bottom) at 1 mM in 0.1 M $\text{TEABF}_4 / \text{ACN}$. **(a)** First positive couple of each active species with ~ 0.7 mM ferrocene internal reference. **(b)** Full potential window of the organic active species, indicating additional irreversible couples at 0.8 – 1.0 V vs. Fc/Fc^+ .

4.2 Cyclic-Voltammetry Scan-Rate Study

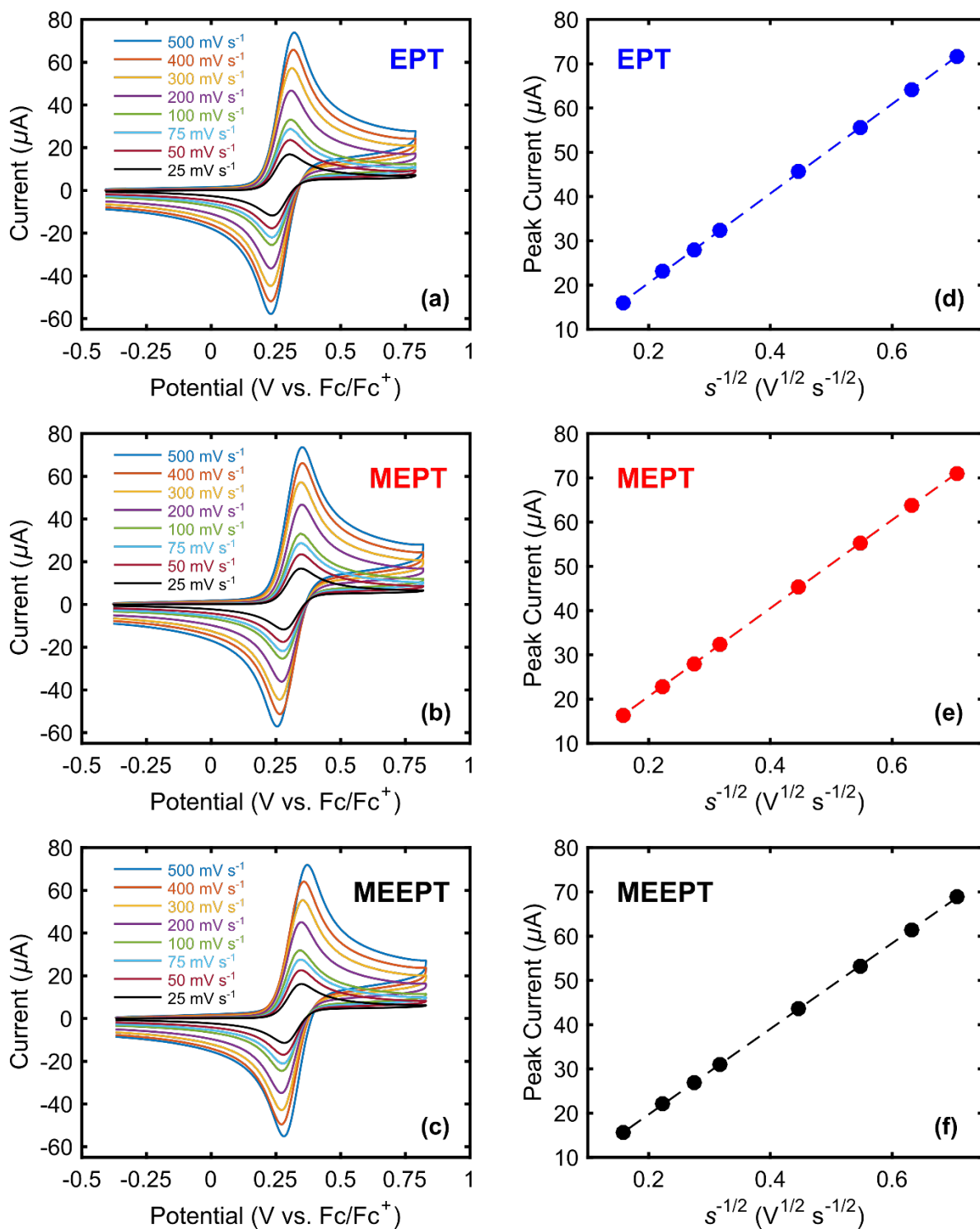


Figure S9. CV scan-rate dependence study for (a) EPT, (b) MEPT, and (c) MEEPT, and Randles-Sevcik construction (peak current vs. square root of scan rate) for the oxidative (anodic) waves of (d) EPT, (e) MEPT, and (f) MEEPT.

5 Bulk Electrolysis

5.1 Bulk-Electrolysis Cell Schematic

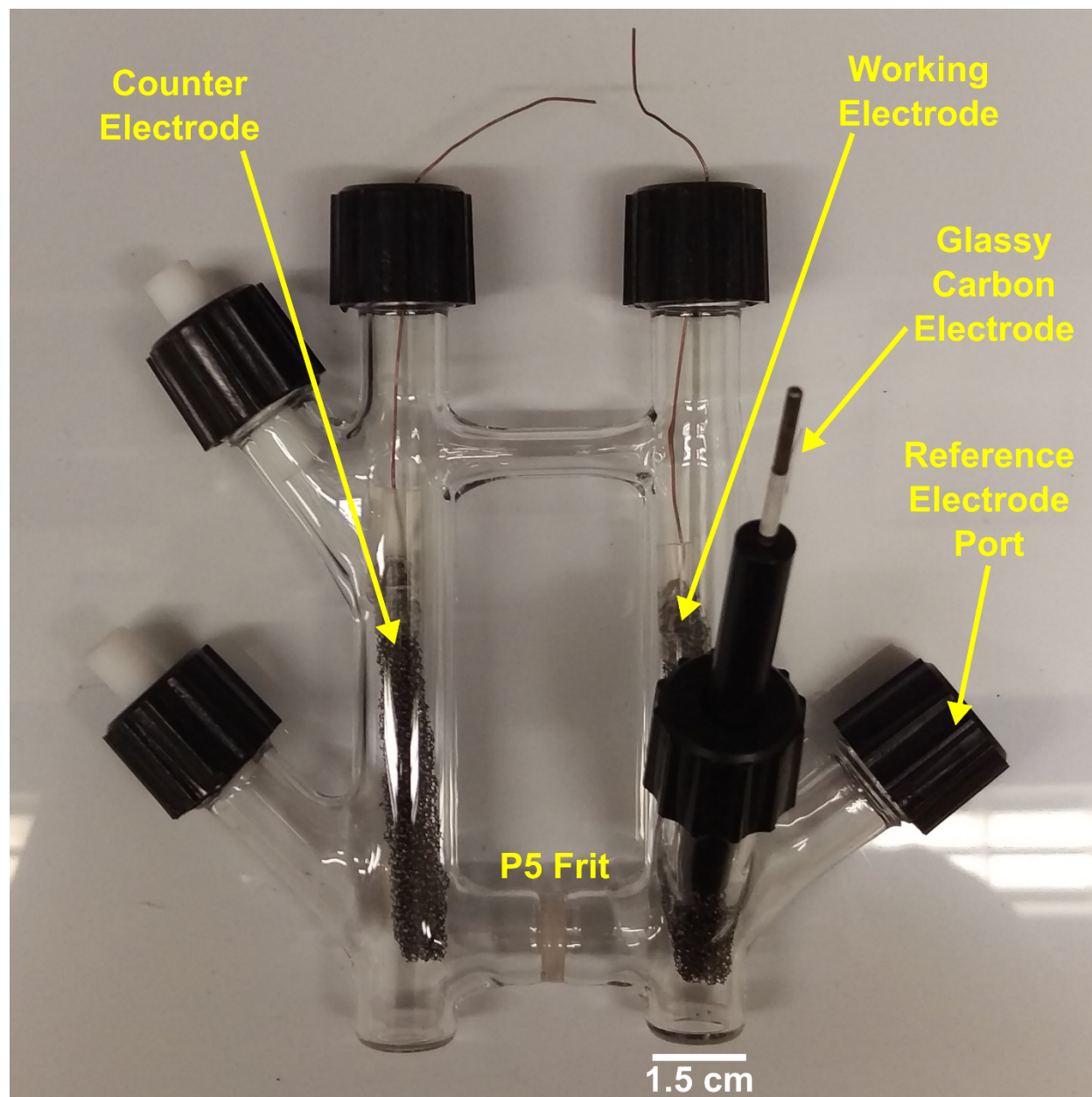


Figure S10. Photograph of the bulk-electrolysis cell, with relevant ports and electrodes labeled.

5.2 Potential vs. Capacity

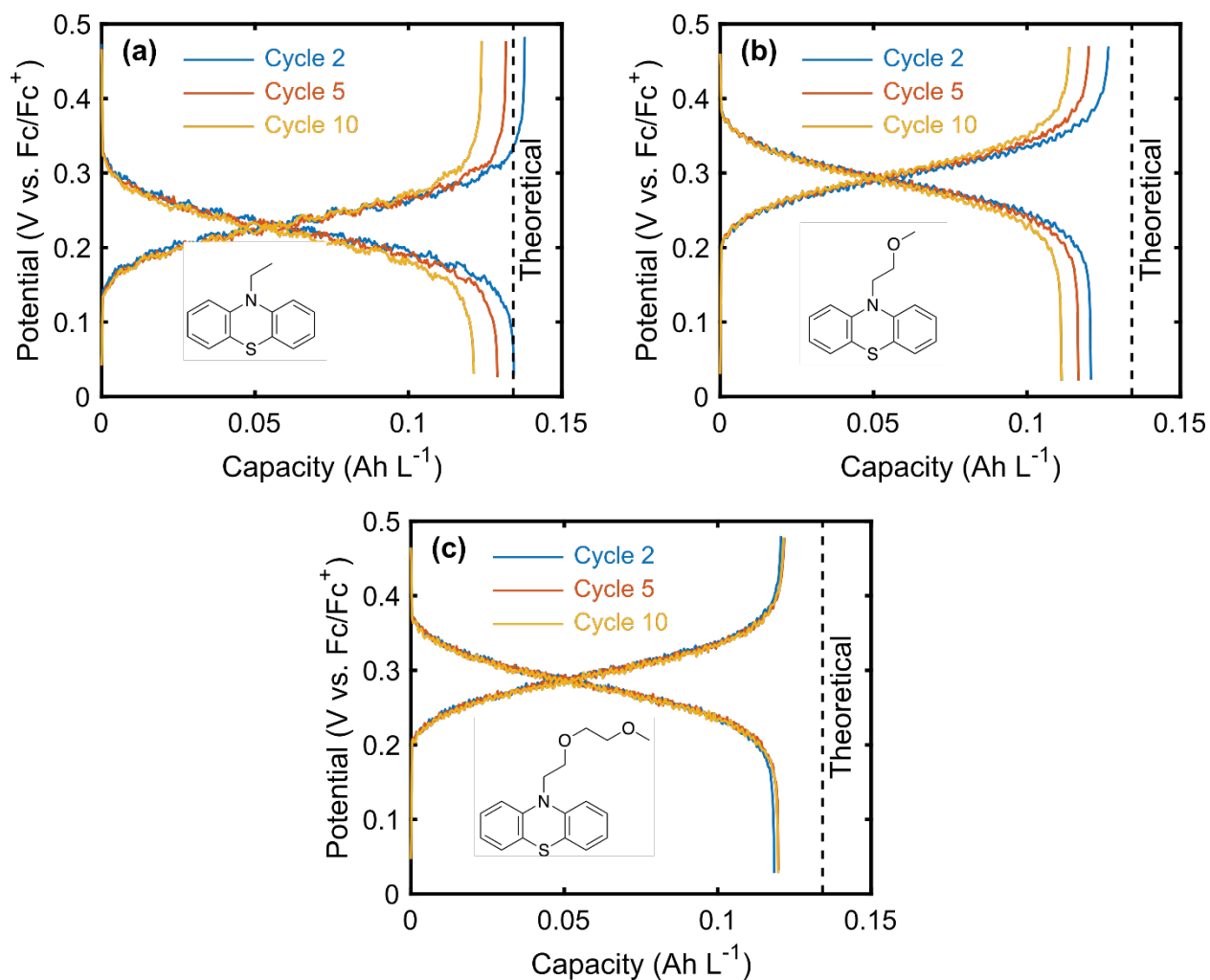


Figure S11. Potential vs. capacity curves from bulk-electrolysis experiments showing cycles 2, 5, and 10 for each of (a) EPT, (b) MEPT, and (c) MEEPT at 5 mM in 1 M TEABF₄ / ACN. Theoretical capacities are 0.134 Ah L⁻¹ (0.469 mAh) for each experiment, and 10 cycles completed in 7 h.

5.3 Cyclic Voltammograms Before and After Cycling

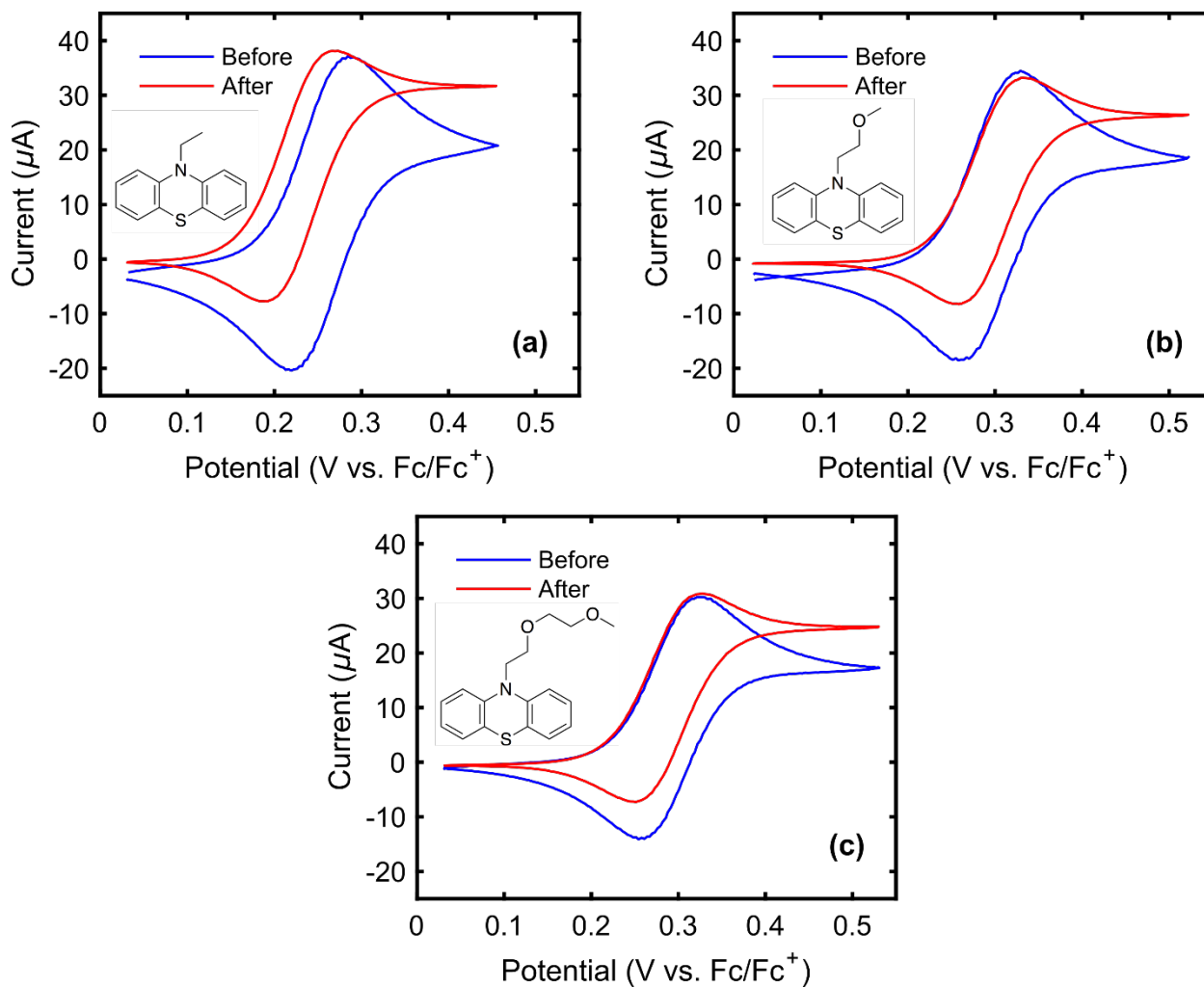


Figure S12. Cyclic voltammograms (cycle 2) before and after 10 bulk-electrolysis cycles for (a) EPT, (b) MEPT, and (c) MEEPT at 5 mM in 1 M $\text{TEABF}_4 / \text{ACN}$.

5.4 Quantitative Cyclic Voltammetry Analysis Before and After Cycling

Table S1: Quantitative CV characteristics of EPT, MEPT, and MEEPT before and after bulk electrolysis cycling. Tabulated values are calculated from the data available in Figure S12.

| | Compound | $E_{1/2}^{0/+}$ (V vs. Fc/Fc⁺) | Peak Separation (mV) | Peak Current Ratio | Peak Oxidative Current (μA) |
|-------------------------------------|-----------------|---|-------------------------------------|-----------------------------------|---|
| <i>Before Bulk Electrolysis</i> | EPT | 0.284 | 65 | 1.050 | 34.7 |
| | MEPT | 0.327 | 63 | 1.072 | 33.9 |
| | MEEPT | 0.327 | 63 | 0.991 | 28.7 |
| <i>After Bulk Electrolysis</i> | EPT | 0.261 | 78 | 0.964 | 36.8 |
| | MEPT | 0.327 | 70 | 1.005 | 33.2 |
| | MEEPT | 0.324 | 76 | 1.004 | 30.5 |

6. Image of Assembled Flow Cell

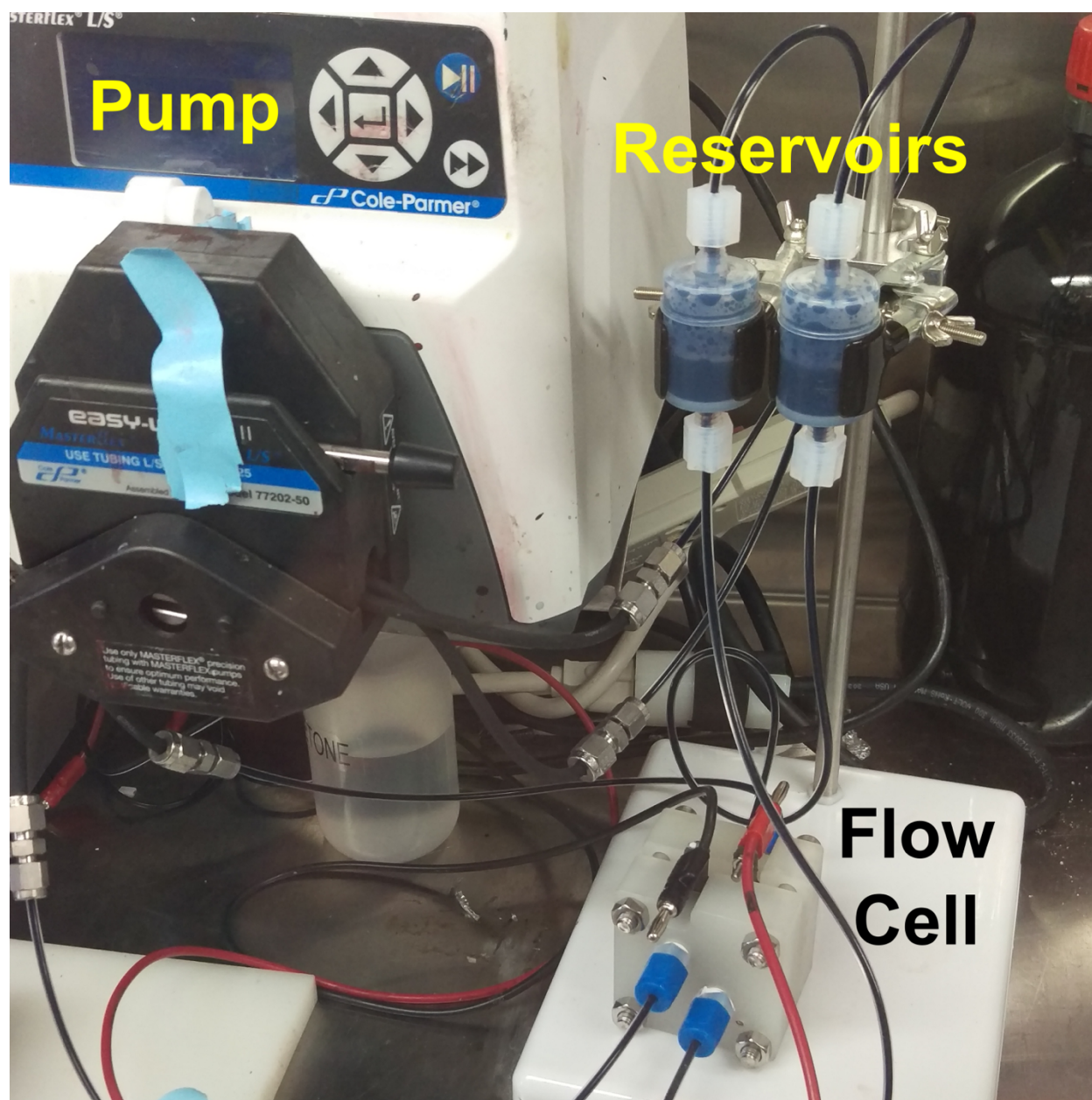


Figure S13. Photograph of the assembled flow cell, connected to the pump and reservoirs.